NJC

PAPER

View Article Online
View Journal | View Issue

Published on 12 February 2018. Downloaded by Argonne Research Library on 8/24/2022 5:34:32 PM.

Check for updates

Cite this: *New J. Chem.*, 2018, **42**, 7796

The complexation and thermodynamics of neptunium(v) with acetate in aqueous solution†

Martin M. Maiwald, *[ab] Andrej Skerencak-Frech[ab] and Petra J. Panak[ab]

Received 12th December 2017,
Accepted 12th February 2018

DOI: 10.1039/c7nj04916a

rsc.li/njc

The complexation of NpO_2^+ with acetate is studied in aqueous solution by absorption spectroscopy as a function of the total ligand concentration (NaAc), ionic strength (I_m = 0.5–4.0 mol kg^{-1} $Na^+(Cl^-/ClO_4^-)$) and temperature (T = 20–85 °C). Three distinct Np(v) species $(NpO_2(Ac)_n^{1-n}$; n = 0, 1, 2) are identified, and their molar fractions determined by peak deconvolution of the absorption spectra. With increasing temperature the molar fractions of the higher complex species increase. The conditional stability constants $\log \beta_j'(T)$ are calculated for each temperature and extrapolated to IUPAC reference state conditions (I_m = 0) using the specific ion interaction theory (SIT). The $\log \beta_n^0(T)$ values increase by approximately 0.4–0.5 logarithmic unit for $NpO_2(Ac)$ and by about 0.5–0.6 for $NpO_2(Ac)_2^-$. Furthermore, the thermodynamic stability constants are linearly correlated with the reciprocal temperature. Thus, fitting the data according to the integrated Van't Hoff equation yields the standard reaction enthalpy $\Delta_r H^0$ and entropy $\Delta_r S^0$ for the complexation reactions. Both complexation reactions are endothermic and driven by the entropy. In addition, the SIT specific binary ion–ion interaction coefficients of the complex species with Na^+/ClO_4^- and Na^+/Cl^- ($\varepsilon_T(i,k)$) are determined as a function of temperature.

Introduction

The safe disposal of highly active nuclear waste, which accumulates by the use of nuclear fission for electrical power generation, is still a pressing problem. Worldwide it is considered to be disposed in deep geological formations. A well-founded understanding of the geochemical behaviour of the radionuclides is of high importance to model their migration behaviour in the near- and far-field of a repository over long time scales. Besides uranium and fission products the transuranium element plutonium and the minor actinides (Np, Am, Cm) are present in the high-level nuclear waste. Due to their long half-lives they will determine the long-term radiotoxicity of the radioactive waste. Therefore, the actinides are of particular interest in the context of a long-term safety assessment of a nuclear waste repository. One of the most important incident scenarios which have be considered hereby is the intrusion of water into the repository and the subsequent dissolution of the nuclear waste. Besides reactions at the liquid–solid interfaces (*e.g.* dissolution of the waste matrix, sorption processes, *etc.*), complexation reactions in the aqueous phase with available organic and inorganic ligands may alter the geochemical behaviour of the actinides considerably. A comprehensive modelling of the migration behaviour of the actinides requires a detailed description of all relevant reactions based on thermodynamic data like standard-state stability constants ($\log \beta_n^0$), standard reaction enthalpies ($\Delta_r H^0$) and entropies ($\Delta_r S^0$).

For the long-term disposal of high-level nuclear waste geological formations of clay rocks, salt rocks or crystalline formations are in discussion. Natural clay rock formations are investigated in several European countries, *i.e.* Belgium,[3] France,[5] Germany[6] and Switzerland.[8] In the pore waters of different clay rock formations dissolved organic compounds (DOC) are present, consisting of large fractions of low molecular weight organic compounds (LMWOC) (*i.e.* Callovo-Oxfordian (COX): 88% LMWOC, Opalinus Clay (OPA): 36% LMWOC).[9–12] Among the different LMWOC acetate is the most abundant compound, with concentrations up to 203 μM in OPA and 1865 μM in COX.

The early actinides U – Am are redox active metals and exist in aqueous solution as An(III) to An(VI) within the thermodynamic stability field of water. The highest mobility in geochemical systems is usually attributed to the pentavalent oxidation state An(v) due to its weak sorption behaviour and high solubility.[14–16] The pentavalent Np(v) is the thermodynamically most stable within the An(v) series.[17–19] It is stable over a wide range of E_h and pH conditions, including certain conditions in the near- and far-field of a nuclear waste repository.[20–25] Nonetheless, Np(v) is not only a key actinide oxidation state in suboxic and oxic repository considerations but also in near-surface contamination where actinides and organics are often co-disposed.

Only a limited number of studies on the complexation of Np(v) with acetate are available in the literature.[1,2,4,7,26,27] A

[a] *Ruprecht Karls Universität Heidelberg, Physikalisch-Chemisches Institut, Im Neuenheimer Feld 253, D-69120 Heidelberg, Germany. E-mail: m.maiwald@pci.uni-heidelberg.de*
[b] *Karlsruher Institut für Technologie (KIT), Institut für Nukleare Entsorgung (INE), D-76344 Eggenstein-Leopoldshafen, Germany*

† Electronic supplementary information (ESI) available. See DOI: 10.1039/c7nj04916a

 This journal is © The Royal Society of Chemistry and the Centre National de la Recherche Scientifique 2018

Published on 12 February 2018. Downloaded by Argonne Research Library on 8/24/2022 5:34:32 PM.

comparison of these studies shows controversial results regarding the speciation of the Np(v)-acetate complexes. Depending on the used experimental approach (spectrophotometry or solvent extraction) a different number of species ($NpO_2(Ac)_n^{1-n}$, n = 1–3) is observed at comparable experimental conditions. Furthermore, the reported stability constants differ considerably and thermodynamic functions at IUPAC reference state conditions are not available.

Thus, the present work focuses on the complexation of NpO_2^+ with acetate to clarify the speciation and to determine thermodynamic functions of the complexation reactions. The complexation is studied in $NaClO_4$ and NaCl solutions by absorption spectroscopy in the near-IR region as a function of temperature (T = 20–85 °C). Application of the specific ion interaction theory (SIT) and the integrated Van't Hoff equation yields the temperature dependent standard-state stability constants ($\log \beta_n^0(T)$) and thermodynamic functions $\Delta_r H^0$ and $\Delta_r S^0$ of the different complexation reactions. Also the binary ion–ion interaction parameters $\varepsilon_T(i,k)$ of the different Np(v) species with Na^+ and Cl^-/ClO_4^- are determined.

Experimental section

Sample preparation

All solutions were prepared on the molar concentration scale (mol kg^{-1} H_2O; "m") to avoid changes of the concentrations due to changes in temperature and/or ionic strength. All chemicals were analytical grade or higher and purchased from Merck Millipore or Alfa Aesar. The samples were prepared using ultrapure water (Milli-Q academic, Millipore). A 4.18×10^{-2} mol kg^{-1} $^{237}Np(v)$ stock solution in 7.0×10^{-2} mol kg^{-1} $HClO_4$ was used to set the total initial Np(v) concentration of the samples to 2.5×10^{-4} mol kg^{-1} in H_2O.[28] The oxidation state and concentration of the Np(v) stock solution was determined by absorption spectroscopy. The total proton concentration of the samples was adjusted to $[H]_{total}^+ = 1.2 \times 10^{-5}$ mol kg^{-1} with $HClO_4$. One series of samples was prepared using a fixed ionic strength (I_m = 4.0 mol kg^{-1} $NaClO_4$) at increasing acetate concentrations. The acetate concentration of the samples was increased by successive titration with a solution of $[NaAc]_{tot}$ = 1.0 mol kg^{-1} at I_m = 4.0 mol kg^{-1} $Na(ClO_4^-/Ac^-)$ and $[NaAc]_{tot}$ = 4.0 mol kg^{-1}. Therefore, the appropriate amount of solid NaAc and $NaClO_4$ was dissolved in water. Furthermore, two additional series of samples were prepared at fixed ligand concentrations and increasing concentrations of $NaClO_4$ or NaCl, respectively. The acetate concentrations were set to $[Ac^-]_{tot}$ = 0.05; 0.11 mol kg^{-1} by dissolving solid NaAc. The concentration of $NaClO_4$ was adjusted by addition of aliquots of an aqueous 13.9 mol kg^{-1} $NaClO_4$ solution. The NaCl ionic strength was increased by addition of solid NaCl into the samples. A detailed summary of the sample compositions is given in the ESI.†

Spectrophotometry

Spectrophotometric titrations in the near-IR region were conducted between 20 to 85 °C using a Varian Cary-5G UV/Vis/NIR spectrophotometer. The temperature of the sample holder inside the spectrophotometer was controlled using a Lauda Eco E100 thermostatic system (temp. accuracy: ±0.5 °C) operated with water as bath liquid. The cuvettes (quartz glass with air tight screw caps, 1 cm path length, Hellma Analytics) were pre-equilibrated at the different temperatures in an external custom-made copper sample holder placed on a heating plate with thermostatic control (VWR Collection VMS-C4 Advanced with IKA (JANKE & KUNKEL) PT 1000 temperature sensor; temp. accuracy: ±0.5 °C). Both thermostatic setups are calibrated with a precision laboratory thermometer filled with mercury (Amrell GmbH & Co. KG, DIN 12775; temp. accuracy: ±0.5 °C) to confirm the correct temperature of the aqueous solution in the cuvettes during measurement. Each sample was equilibrated 15 min at the respective temperature to ensure chemical equilibrium before measurement. Spectra were recorded with data intervals of 0.1 nm, a scan rate of 60 nm min^{-1} (ave. time: 0.1 s) and a slit width of 0.7 nm in double beam mode. Separate baselines are recorded for each temperature, ionic strength condition and ligand concentration.

Results and discussion

Absorption spectra

The absorption spectra of Np(v) at T = 20 and 85 °C, and I_m = 4.0 mol kg^{-1} $NaClO_4$ are displayed in Fig. 1 as a function of the total ligand concentration. At 20 °C the Np(v) aquo ion shows an absorption band at 979.5 nm which is in excellent agreement with the literature.[29] The absorption is hypsochromically shifted by 0.7 nm compared to $I_m < 0.5$ mol kg^{-1}.[30,31] The shift of the absorption band with the ionic strength is already described in the literature.[29,32] With increasing acetate concentration the absorption band shifts to higher wavelengths and two isosbestic points are visible at 983.7 and 986.0 nm, indicating the formation of two different Np(v) acetate complexes. Furthermore, the Full Width at Half Maximum (FWHM) of the absorption bands increases from 7.3 to 12.3 nm with increasing $[Ac^-]_{tot}$. At elevated temperature (T = 85 °C, Fig. 1 (bottom)) the absorption spectrum of the Np(v) aquo ion is hypsochromically shifted by 1.7 nm to 977.8 nm. The FWHM is unaffected by the temperature and remains at 7.3 nm. With increasing ligand concentration the Np(v) absorption band also shifts bathochromically to higher wavelengths. However, only one isosbestic point is observed, which is located at 981.6 nm at 85 °C. The position of the isosbestic point is shifted by 1.6 nm towards lower wavelengths compared to 20 °C, reflecting the general hypsochromic shift of the Np(v) band with increasing temperature. The increase in the FWHM from 7.3 to 12.8 nm is slightly more pronounced at elevated temperature. At each temperature the bathochromic shift of the absorption band clearly indicates the formation of $NpO_2(Ac)_n^{1-n}$ complexes, which is fostered at increased temperature indicating an endothermic complexation behaviour. The temperature induced hypsochromic shift of the absorption band of Np(v) is contrary to the bathochromic shift of the spectra resulting from the complexation of Np(v). It is known that temperature and ionic strength significantly affect the absorption of Np(v) in aqueous solution.[29,32]

Published on 12 February 2018. Downloaded by Argonne Research Library on 8/24/2022 5:34:32 PM.

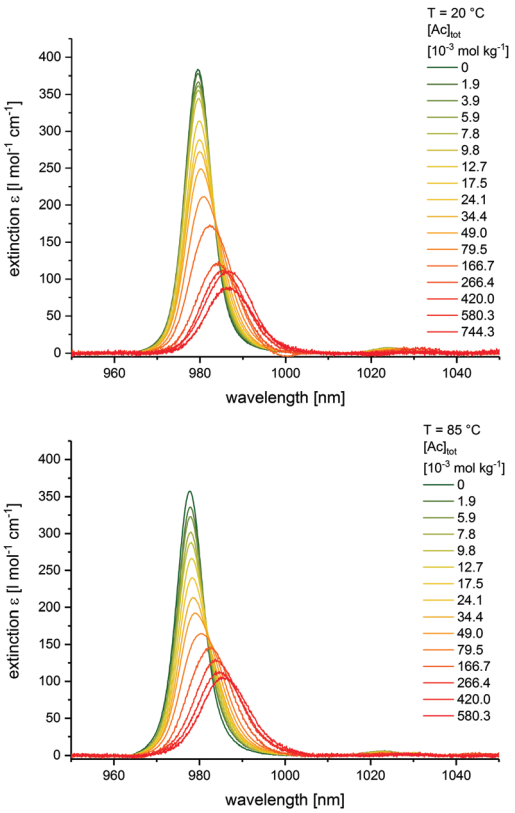


Fig. 1 Absorption spectra of Np(v) as a function of the total acetate $[Ac]_{tot}$ concentration at T = 20 °C (top), and T = 85 °C (bottom) and I_m ($NaClO_4$) = 4.0 mol kg^{-1}.

The hypsochromic shift is explained by solvatochromic effects.[33–37] The temperature and ionic strength influence the physical properties of water like the dielectric constant, refractive index and polarity.[38,39] This results in changes in the electronic absorption of Np(v). Furthermore, they also affect the solvation of Np(v) in the second hydration sphere which results in additional changes of the spectroscopic properties.[32] Due to the temperature- and ionic strength dependence of the absorption bands, each series of spectra has to be treated separately and single component spectra have to be determined for all studied experimental temperature and ionic strength conditions.

Peak deconvolution and speciation

The pure component spectra of the complexed species $NpO_2(Ac)$ and $NpO_2(Ac)_2^-$ are derived *via* subtractive peak deconvolution at each temperature condition using the absorption spectrum of the Np(v) aquo ion obtained from $NaClO_4$ solution at the respective temperature. Hereby, identical spectra for $NpO_2(Ac)$ and $NpO_2(Ac)_2^-$ are determined in NaCl and $NaClO_4$ media at equal ionic strength and temperature. Thus, a complexation of Cl^- at high NaCl ionic strengths can be excluded. The results for 20 and 85 °C are presented in Fig. 2. Additionally, all single component spectra are given in the ESI.† At 20 °C the absorption band of $NpO_2(Ac)$ is located at λ_{max} = 984.2 nm (ε = 192 ± 9 L mol^{-1} cm^{-1}, λ_{FWHM} = 8.9 ± 0.4 nm) and is bathochromically shifted by 4.7 nm compared to the Np(v) aquo ion. The absorption

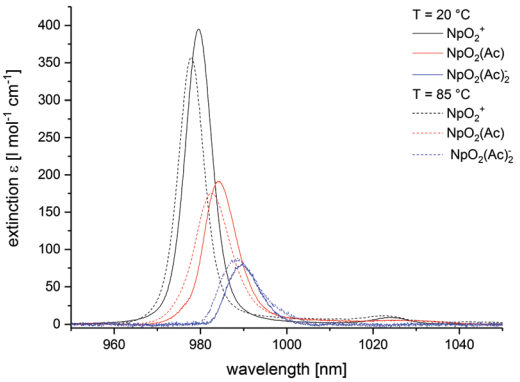


Fig. 2 Absorption spectra of the Np(v) aquo ion and the $NpO_2(Ac)_n^{1-n}$ (n = 1, 2) complexes at 20 °C (solid lines) and 85 °C (dashed lines) (I_m($NaClO_4$) = 4.0 mol kg^{-1}).

maximum of $NpO_2(Ac)_2^-$ is observed at λ_{max} = 989.6 nm (ε = 80 ± 4 L mol^{-1} cm^{-1}, λ_{FWHM} = 8.6 ± 0.4 nm), corresponding to a bathochromic shift of 10.1 nm. With increasing temperature all absorption bands of the different Np(v) complex species are hypsochromically shifted by 1.6 nm. Nonetheless, the temperature does not influence the integrated absorption coefficients of the absorption bands and changes of the molar attenuation coefficient and FWHM are within in the error range of the deconvolution. This shows that the T and I_m induced blue shift is independent of the chemical speciation and results from changes in the absorption properties of the Np(v) ion. The position of the absorption band of $NpO_2(Ac)$ at room temperature determined in the present work is in excellent agreement with literature data.[1] However, the extinction coefficient (ε = 191 ± 7 L mol^{-1} cm^{-1}) is lower compared to the value in the literature ($\varepsilon \approx$ 320 L mol^{-1} cm^{-1}). A comparison of the absorption spectrum of $NpO_2(Ac)$ with that of the analogous 1 : 1 Np(v)–propionate complex (λ_{max} = 984 nm, ε = 180 ± 10 L mol^{-1} cm^{-1}) shows that the spectroscopic properties are in excellent agreement.[13] This is due to the similar chemical and electronic structure of both ligands. The deconvolution of the experimental absorption spectra is performed by principle component analysis using the pure component spectra.[40,41]

The speciation of the Np(v) acetate system (symbols) is displayed in Fig. 3 as a function of the equilibrium acetate concentration at T = 20 and 85 °C and I_m = 4.0 mol kg^{-1} $NaClO_4$. Also, the calculated speciations (lines) using the derived log $\beta_n'(T)$ values (see next section) are given. The species distributions for all studied experimental conditions are given in the ESI.† With increasing ligand concentration the chemical equilibrium is shifted towards the complexed species. At 20 °C and $[Ac^-]_{eq} > 5 \times 10^{-2}$ mol kg^{-1} $NpO_2(Ac)$ dominates the species distribution. For $[Ac^-]_{eq} > 3.6 \times 10^{-1}$ mol kg^{-1} the $NpO_2(Ac)_2^-$ complex becomes the dominant species. The comparison of the species distributions at 20 and 85 °C clearly shows that at equal ligand concentrations the mole fractions of the complex species are increased at higher temperature. At 85 °C the $NpO_2(Ac)$ complex is the dominant species at $[Ac^-]_{eq} > 2 \times 10^{-2}$ mol kg^{-1} and $NpO_2(Ac)_2^-$ prevails at $[Ac^-] > 3.2 \times 10^{-1}$ mol kg^{-1}.

 This journal is © The Royal Society of Chemistry and the Centre National de la Recherche Scientifique 2018

Published on 12 February 2018. Downloaded by Argonne Research Library on 8/24/2022 5:34:32 PM.

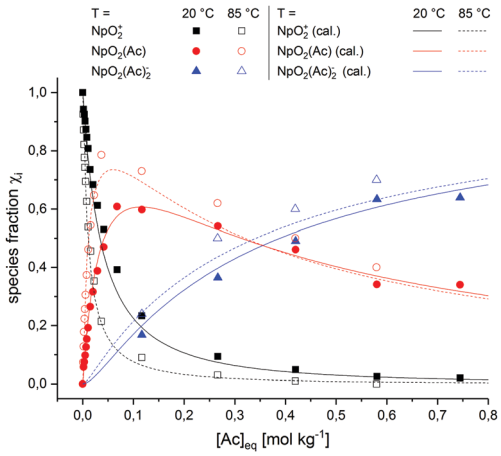


Fig. 3 Experimental (symbols) and calculated (lines) species distribution of $NpO_2(Ac)_n^{1-n}$ (n = 0, 1, 2) complexes as a function of the equilibrium ligand concentration in aqueous solution. $I_m(NaClO_4)$ = 4.0 mol kg^{-1}; T = 20 °C (solid lines) and 85 °C (dashed lines). Calculations with log β_1(20 °C) = 1.43 ± 0.09, log β_2(20 °C) = 1.88 ± 0.12, log β_1(85 °C) = 1.97 ± 0.15, log β_2(85 °C) = 2.45 ± 0.16.

The single component spectra and the experimentally determined speciation are verified by slope analysis at each studied temperature. The slope analyses are performed according to eqn (1):

$$\log \beta_n' = \log \frac{[NpO_2(Ac)_n]^{1-n}}{[NpO_2]^+} - n \log[Ac^-]_{eq} \qquad (1)$$

with $[Ac^-]_{eq}$ being the free, deprotonated acetate concentration in solution at a given temperature. $[Ac^-]_{eq}$ is calculated for each temperature according to literature procedure using the Henderson–Hasselbalch equation, SIT and temperature dependent pK_a^0 values.[42–44] In Fig. 4 the slope analyses at I_m = 4.0 mol kg^{-1} are displayed for 20 and 85 °C. The results show that the logarithm of the mole fractions $\log(NpO_2(Ac)_n^{1-n}/NpO_2(Ac)_{n-1}^{2-n})$ correlate linearly with $\log([Ac^-]_{eq})$. The exclusive formation of the two Np(v)-acetate complex species with stoichiometries of $NpO_2(Ac)_n^{1-n}$ (n = 1, 2) are confirmed at all experimental conditions (see ESI,† for the results of all slope analyses). This differs from the results obtained by Takao *et al.* using absorption spectroscopy and EXAFS.[26] The authors report the formation of $NpO_2(Ac)_n^{1-n}$ (n = 1–3) in a concentration range of $[Ac^-]_{eq} \approx$ 0–1 mol L^{-1}, which is almost identical to that of the present work. On the contrary, in a further spectroscopic study performed by Rao *et al.* the formation of only $NpO_2(Ac)$ up to $[Ac^-]_{total} \leq$ 0.3 mol L^{-1} is reported.[1] This is supported by various solvent extraction studies also providing only the formation of $NpO_2(Ac)$ up to $[Ac^-]_{total} \leq$ 0.2 mol L^{-1}. Furthermore, the results of the present work are compared to that of Np(v) with propionate (Prop).[13] In a concentration range up to $[Prop^-]_{total} \leq$ 0.1 mol kg^{-1} the formation of $NpO_2(Prop)$ is confirmed in the temperature range of 20–85 °C. This is in very good agreement with the observations in the present work with mole fractions of $NpO_2(Ac)_2^-$ being negligible for $[Ac^-]_{eq} \leq$ 0.1 mol kg^{-1}. Due to the limited $[Prop^-]_{eq}$ concentration the formation of $NpO_2(Prop)_2^-$ was not observed.

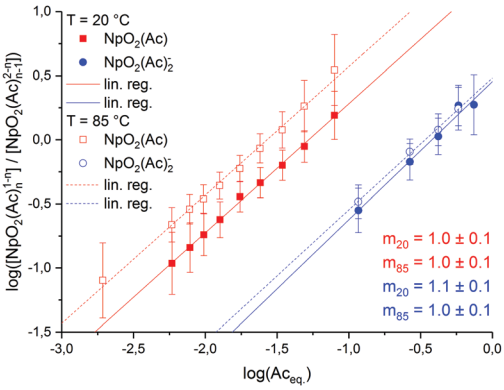


Fig. 4 Plots of log $([NpO_2(Ac)_n]^{1-n}/[NpO_2(Ac)_{n-1}]^{2-n})$ *vs.* log$([Ac^-]_{eq})$ and linear regression analyses at 20 and 85 °C ($I_m(NaClO_4)$ = 4.0 mol kg^{-1}). Due to minimization of the error, data points with at least one Np(v) species below 5% are omitted in the slope analyses.

Thermodynamic data

The log $\beta_n'(T)$ values for the formation of $NpO_2(Ac)$ and $NpO_2(Ac)_2^-$ are calculated according to the law of mass action (eqn (1)) using the determined speciation and the equilibrium acetate concentrations. The conditional stability constants are extrapolated to I_m = 0 with the specific ion interaction theory (SIT) as recommended by the NEA-TDB (see ESI,† for more information).[17,18] The log $\beta_n^0(T)$ values are summarized in Table 1. The thermodynamic stability constants log $\beta_n^0(T)$ obtained in NaCl and $NaClO_4$ media are in good agreement within the error range. Hence, averaged values for log $\beta_n^0(T)$ are calculated, yielding log β_1^0(20 °C) = 1.31 ± 0.18 for NpO_2Ac and log β_2^0(20 °C) = 1.35 ± 0.17 for $NpO_2(Ac)_2^-$. With increasing temperature the first stability constant increases by approximately 0.5 logarithmic units to log β_1^0(85 °C) = 1.80 ± 0.16 and the second increases by 0.6 to log β_2^0(85 °C) = 1.96 ± 0.21.

To determine the standard reaction enthalpy $\Delta_r H_{0n,m}^0$ and entropy $\Delta_r S_{0n,m}^0$ the averaged log $\beta_n^0(T)$ are plotted *versus* the reciprocal temperature T^{-1} (see Fig. 5). The data correlate linearly with T^{-1} and the temperature dependence is thus well described by the integrated van't Hoff equation (eqn (2)).

$$\log K_n^0(T) = \log K_n^0(T_0) + \frac{\Delta_r H_m^0(T_0)}{R \ln(10)} \left(\frac{1}{T_0} - \frac{1}{T} \right) \qquad (2)$$

R is the universal gas constant and T the absolute temperature. T_0 = 298.15 K and is the temperature of the IUPAC reference state. The equation is valid in the studied temperature range of 20–85 °C, assuming $\Delta_r C_{m,p}^0$ = 0 and $\Delta_r H_m^0$ = const. The $\Delta_r H_{0n,m}^0$ and $\Delta_r S_{0n,m}^0$ values determined in the present work are summarized in Table 2. The reaction enthalpies and entropies are positive. Averaged values of $\Delta_r H_{01,m}^0$ ($NpO_2(Ac)$)= 14.8 ± 1.6 kJ mol^{-1} and $\Delta_r H_{02,m}^0$ ($NpO_2(Ac)_2^-$)= 19.0 ± 2.1 kJ mol^{-1} are obtained. The standard reaction entropies are $\Delta_r S_{01,m}^0(NpO_2(Ac))$ = 74 ± 10 J mol^{-1} K^{-1} and $\Delta_r S_{02,m}^0(NpO_2(Ac)_2^-)$ = 89 ± 16 J mol^{-1} K^{-1}. Thus, the formation of $NpO_2(Ac)$ and $NpO_2(Ac)_2^-$ is driven by the high gain of entropy.

For comparison with literature data log β_1^0(25 °C) is calculated using the integrated Van't Hoff equation (eqn (2)). A comparison of log β_1^0(25 °C) with literature data is given in Table 3.

Published on 12 February 2018. Downloaded by Argonne Research Library on 8/24/2022 5:34:32 PM.

Table 1 Thermodynamic stability constants $\log \beta_n^0(T)$ for the formation of $[NpO_2(Ac)_n]^{1-n}$ (n = 1, 2) obtained in $NaClO_4$ and NaCl media as a function of the temperature. Errors correspond to the uncertainty of $\pm 3\sigma$ (99.7% level of confidence)

	T [°C]	20	30	40	50	60	70	80	85
$[NpO_2(Ac)]$	$NaClO_4$	1.29 ± 0.12	1.38 ± 0.12	1.43 ± 0.11	1.48 ± 0.11	1.60 ± 0.12	1.72 ± 0.12	1.74 ± 0.12	1.82 ± 0.11
	NaCl	1.33 ± 0.13	1.38 ± 0.13	1.43 ± 0.12	1.51 ± 0.12	1.61 ± 0.12	1.66 ± 0.12	1.67 ± 0.12	1.77 ± 0.12
	∅	1.31 ± 0.18	1.38 ± 0.18	1.43 ± 0.16	1.50 ± 0.16	1.61 ± 0.17	1.69 ± 0.17	1.71 ± 0.17	1.80 ± 0.16
$[NpO_2(Ac)_2]^-$	$NaClO_4$	1.36 ± 0.12	1.49 ± 0.13	1.56 ± 0.13	1.61 ± 0.12	1.75 ± 0.14	1.89 ± 0.12	1.91 ± 0.12	2.01 ± 0.13
	NaCl	1.34 ± 0.13	1.34 ± 0.16	1.44 ± 0.16	1.54 ± 0.16	1.68 ± 0.19	1.75 ± 0.19	1.79 ± 0.17	1.91 ± 0.17
	∅	1.35 ± 0.17	1.42 ± 0.21	1.50 ± 0.21	1.58 ± 0.20	1.72 ± 0.24	1.82 ± 0.22	1.85 ± 0.21	1.96 ± 0.21

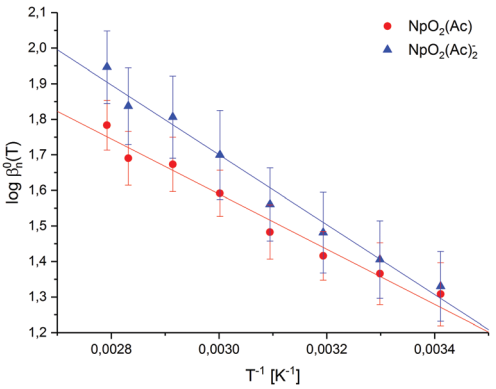


Fig. 5 Plot of $\log \beta_n^0(T)$ (n = 1, 2) as a function of the reciprocal temperature and fitting according to the integrated Van't Hoff equation. The error bars equal the uncertainty of $\pm 3\sigma$ (99.7% level of confidence).

Spectrophotometric studies on the Np(v) complexation with acetate by Rao *et al.* provide $\log \beta_1^0(25\ ^\circ C) = 1.05 \pm 0.04$.[1] This value is by 0.24 logarithmic units lower compared to the stability constants of the present work. Moore *et al.*, Novak *et al.* and Pokrovsky *et al.* obtained $\log \beta_1^0(25\ ^\circ C)$ values in the range of 1.30–1.46, determined by solvent extraction.[2,4,7] The reported thermodynamic stability constants are in excellent agreement with that of the present work. The formation of higher complex species is not observed in these studies.

Furthermore, the stability constant of the $NpO_2(Ac)$ complex in the present work is in excellent agreement with the value of the analogue $NpO_2(Prop)$ complex ($\log K_{25^\circ C}^0(NpO_2(Prop)) = 1.26 \pm 0.03$).[13] This is due to the similar chemical properties of acetic and propionic acid. Both carboxylic acids have similar pK_a^0 values and the coordinating functional group is identical. The effect of the alkyl backbone on the complex stability is negligible as it has only a minor impact on the electron density at the carboxylic group.

Table 3 Thermodynamic stability constants for the complexation of Np(v) with acetate and propionate at 25 °C, p.w. = present work, sp = spectrophotometry, sx = solvent extraction, cal = microcalorimetry

	Method	Electrolyte	$\log \beta_{25^\circ C}^0$	Ref.
$[NpO_2(Ac)]$	sp	$NaClO_4$	1.31 ± 0.14	p.w.
	sp	NaCl	1.34 ± 0.14	p.w.
	sp, cal	$NaClO_4$	1.05 ± 0.04	RAO10[1]
	sx	$NaClO_4$	1.35	POK97[2]
	sx	NaCl	1.46 ± 0.22	NOV96[4]
	sx	NaCl	1.30 ± 0.06[a]	MOO78[7]
$[NpO_2(Ac)_2]^-$	sp	$NaClO_4$	1.38 ± 0.26	p.w.
	sp	NaCl	1.32 ± 0.29	p.w.
$[NpO_2(Prop)]$	sp	NaCl	1.26 ± 0.03	VAS15[13]

[a] Calculated from literature data.

The comparison of the standard reaction enthalpies and entropies for the complexation of Np(v) with acetate with literature data is not possible due to the lack of literature values at IUPAC reference state. Nonetheless, they can be compared to data of the Np(v) propionate system. The formation of $NpO_2(Prop)$ is also endothermic with $\Delta_r H_m^0 = 10.9 \pm 1.2$ kJ mol^{-1} and driven by the entropy ($\Delta_r S_m^0 = 62 \pm 4$ J mol^{-1} K^{-1}). The thermodynamic functions are in good agreement with those of the present work.

Rao *et al.* determined the conditional reaction enthalpy and entropy for the formation of $NpO_2(Ac)$ at I_m = 1.05 mol kg^{-1} Na(ClO_4/Ac) using calorimetric titrations.[1] The results show $\Delta_r H_m' = 18.1 \pm 1.8$ kJ mol^{-1} and $\Delta_r S_m' = 75 \pm 6$ J mol^{-1} K^{-1}. Both values are in excellent agreement with the conditional values determined in the present work at the same ionic strength ($\Delta_r H_m' = 16.5 \pm 1.5$ kJ mol^{-1}, $\Delta_r S_m' = 73 \pm 8$ J mol^{-1} K^{-1}).

Application of the SIT yields the stoichiometric sum of the binary ion interaction coefficients of the complexation reactions ($\Delta\varepsilon_{01}$ and $\Delta\varepsilon_{02}$). The $\Delta\varepsilon_{01}$ and $\Delta\varepsilon_{02}$ values for the formation of $NpO_2(Ac)_n^{1-n}$ (n = 1, 2) in $NaClO_4$ and NaCl media are displayed in Fig. 6 as a function of the temperature. In $NaClO_4$ medium the $\Delta\varepsilon_n$ values show no temperature dependence whereas $\Delta\varepsilon_{01}$ decreases

Table 2 Thermodynamic data for the formation of $NpO_2(Ac)_n^{1-n}$ (n = 1, 2) according to eqn (1) and (2). Errors correspond to the uncertainty of $\pm 3\sigma$ (99.7% level of confidence)

Electrolyte	$NpO_2(Ac)_n^{1-n}$	$\log \beta_n^0(25\ ^\circ C)$	$\Delta_r H_{0n,m}^0$ [kJ mol^{-1}]	$\Delta_r S_{0n,m}^0$ [J mol^{-1} K^{-1}]	$\Delta\varepsilon$
$NaClO_4$	n = 1	1.29 ± 0.14	15.9 ± 1.3	77 ± 8	−0.18 ± 0.06
	n = 2	1.34 ± 0.14	19.4 ± 1.6	90 ± 12	−0.08 ± 0.03
NaCl	n = 1	1.34 ± 0.26	13.6 ± 1.0	71 ± 6	−0.15 ± 0.06
	n = 2	1.32 ± 0.29	18.6 ± 1.4	87 ± 10	−0.11 ± 0.06
∅	n = 1	1.31 ± 0.27	14.8 ± 1.6	74 ± 10	—
	n = 2	1.33 ± 0.29	19.0 ± 2.1	89 ± 16	—

 This journal is © The Royal Society of Chemistry and the Centre National de la Recherche Scientifique 2018

Published on 12 February 2018. Downloaded by Argonne Research Library on 8/24/2022 5:34:32 PM.

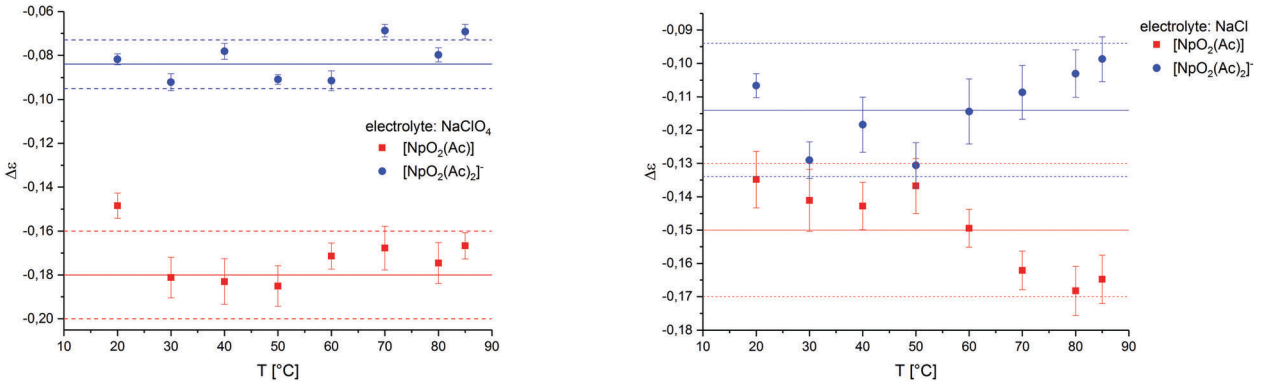


Fig. 6 $\Delta\varepsilon_{0n}$ values for the formation of $[NpO_2(Ac)_n]^{1-n}$ (n = 1, 2) in $NaClO_4$ (left) and NaCl (right) as a function of the temperature. The error bars (dashed lines) equal the 2σ error of the mean values (solid lines) (95.4% level of confidence).

and $\Delta\varepsilon_{02}$ increases slightly in NaCl. However, the temperature dependence is within the error range of the data. Various studies on the ionic strength dependence of the complexation reactions of trivalent lanthanides and actinides as well as recent studies on the Np(v)-sulfate complexation showed, that the effect of temperature on $\Delta\varepsilon_{j,k}$ is rather small and thus negligible in the temperature range of 20 to 90 °C.[13,29,42,45] This applies also to the temperature dependence of $\Delta\varepsilon_{j,k}$ in the present work. Thus, averaged temperature-independent $\Delta\varepsilon_{j,k}$ values are determined for NaCl and $NaClO_4$ as background electrolytes (Table 2). The averaged values are $\Delta\varepsilon_{01} = -0.18 \pm 0.06$ ($NaClO_4$), $\Delta\varepsilon_{01} = -0.15 \pm 0.06$ (NaCl), $\Delta\varepsilon_{02} = -0.08 \pm 0.03$ ($NaClO_4$) and $\Delta\varepsilon_{02} = -0.11 \pm 0.06$ (NaCl). In order to derive the binary ion–ion interaction coefficients $\varepsilon_{j,k}$ of the different Np(v) acetate complexes with Na^+ and Cl^-/ClO_4^- the following parameters given by the NEA-TDB: $\varepsilon(Na^+, Ac^-) = 0.08 \pm 0.01$, $\varepsilon(NpO_2^+, ClO_4^-) = 0.25 \pm 0.05$, and $\varepsilon(NpO_2^+, Cl^-) = 0.09 \pm 0.05$ are used.[17] $\varepsilon(Na^+ + Cl^-/ClO_4^-, NpO_2(Ac))$ and $\varepsilon(Na^+, NpO_2(Ac)_2^-)$ are calculated according to eqn (3) and (4).

$$\log K' - \Delta z^2 D = \log K^0 + \Delta\varepsilon I_m \quad (3)$$

$$\Delta\varepsilon = \sum\varepsilon_{\text{products}} - \sum\varepsilon_{\text{educt}} \quad (4)$$

The obtained vales are $\varepsilon(Na^+ + Cl^-, NpO_2(Ac)) = 0.02 \pm 0.06$, $\varepsilon(Na^+ + ClO_4^-, NpO_2(Ac)) = 0.15 \pm 0.06$ and $\varepsilon(Na^+, NpO_2(Ac)_2^-) = -0.01 \pm 0.06$. In case of an uncharged species $\varepsilon_{i,k}$ is assumed to be zero according to the SIT. In NaCl medium $\varepsilon(Na^+ + Cl^-, NpO_2(Ac),)$ is in good agreement with this assumption, but deviates slightly from zero in $NaClO_4$.

Nonetheless, the obtained $\log\beta_1^0(T)$ values and thermodynamic functions for both electrolytes are in excellent agreement. This confirms that the ionic strength dependence of the complex formation is accurately described using the determined $\varepsilon_{j,k}$ values. The comparison with literature data is not possible as no SIT specific binary ion–ion interaction coefficients are available.

Summary and conclusion

In this work the complexation of Np(v) with acetate is studied systematically as a function of the ligand concentration (Ac^-), ionic strength (NaCl and $NaClO_4$) and temperature (20–85 °C) using absorption spectroscopy. The results show the formation of two different complex species which are identified as $NpO_2(Ac)$ and $NpO_2(Ac)_2^-$ complexes by slope analyses. The formation of higher complexes is not observed under the experimental conditions of $[Ac^-]_{total}$ = 0–1.0 mol kg^{-1} and T_{max} = 85 °C. At elevated temperatures the complexation is more pronounced which is reflected by an increase of the thermodynamic stability constants of both species by 0.5–0.6 orders of magnitude. Correlation of $\log\beta_n^0(T)$ with the reciprocal temperature and fitting according to the integrated Van't Hoff equation yield the standard reaction enthalpies ($\Delta_r H_{0n,m}^0$) and entropies ($\Delta_r S_{0n,m}^0$). $\Delta_r H_{0n,m}^0$ and $\Delta_r S_{0n,m}^0$ are positive confirming that the complexation reactions are endothermic and solely driven by a high gain of entropy. Furthermore, the $\Delta\varepsilon_{01}$ and $\Delta\varepsilon_{02}$ values are determined as a function of temperature for the two different ionic media (NaCl and $NaClO_4$). No significant temperature dependence of $\Delta\varepsilon_{01}$ and $\Delta\varepsilon_{02}$ is observed and thus temperature independent mean values for $\varepsilon(Na^+ + Cl^-/ClO_4^-, NpO_2(Ac))$ and $\varepsilon(Na^+, NpO_2(Ac)_2^-)$ are calculated.

The present work is a detailed spectroscopic study on the complexation of pentavalent Np(v) with acetate in NaCl and $NaClO_4$ media, giving the respective standard state thermodynamic functions $\Delta_r H_{0n,m}^0$, $\Delta_r S_{0n,m}^0$ and $\log\beta_n^0(T)$. A detailed knowledge of the thermodynamics of relevant geochemical processes, like complexation reactions with organic and inorganic ligands in the aqueous phase, is essential to access a model to describe the migration behaviour of actinides under natural conditions over very long time scales. As temperatures highly above 25 °C will be present in the near-field of a repository, thermodynamic data at ambient and at increased temperatures is required for an in-depth understanding of the aqueous geochemistry of actinide elements at conditions relevant for nuclear waste disposal. Thus, the data determined herein are a valuable contribution to the thermodynamic database of actinides improving the scientific basis for accessing nuclear waste disposal scenarios at elevated temperature conditions.

Conflicts of interest

There are no conflicts to declare.

Published on 12 February 2018. Downloaded by Argonne Research Library on 8/24/2022 5:34:32 PM.

Acknowledgements

All spectroscopic measurements were carried out at the Institute for Nuclear Waste Disposal (INE) at Karlsruhe Institute of Technology (KIT). Dr D. Fellhauer and Dr M. Altmaier are acknowledged for providing the ^{237}Np and their experimental support. This work is supported by the German Federal Ministry of Education and Research (BMBF) under Contract 02NUK039C.

References

1 L. Rao, G. Tian, T. G. Srinivasan, P. Zanonato and P. Di Bernardo, *J. Solution Chem.*, 2010, **39**, 1888–1897.
2 O. S. Pokrovsky and G. R. Choppin, *Radiochim. Acta*, 1997, **79**, 167–171.
3 R. Gens, P. Lalieux, P. D. Preter, A. Dierckx, J. Bel, J.-P. Boyazis and W. Cool, *MRS Proceedings*, 2011, **807**, 917–924.
4 C. F. Novak, M. Borkowski and G. R. Choppin, *Radiochim. Acta*, 1996, **74**, 111–116.
5 N. E. A. Oecd, Safety of Geological Disposal of High-level and Long-lived Radioactive Waste in France Nuclear Energy Agency Organisation For Economic Co-Operation And Development, 2006.
6 P. Hoth, H. Wirth, K. Reinhold, V. Bräuer, P. Krull and H. Feldrappe, BGR Bundesanstalt für Geowissenschaften und Rohstoffe, Hannover/Germany, 2007.
7 R. C. Moore, M. Borkowski, M. G. Bronikowski, J. Chen, O. S. Pokrovsky, Y. Xia and G. R. Choppin, *J. Solution Chem.*, 1999, **28**, 521–531.
8 NAGRA, Projekt Opalinuston – Synthese der geowissenschaftlichen Untersuchungsergebnisse, Entsorgungsnachweis für abgebrannte Brennelemente, verglaste hochaktive sowie langlebige mittelaktive Abfälle, NAGRA Nationale Genossenschaft für die Lagerung radioaktiver Abfälle, Wettingen/Switzerland, 2002.
9 E. Gaucher, C. Robelin, J. Matray, G. Negrel, Y. Gros, J. Heitz, A. Vinsot, H. Rebours, A. Cassagnabere and A. Bouchet, *Phys. Chem. Deep Earth*, 2004, **29**, 55–77.
10 T. R. Allen, R. E. Stoller and S. Yamanaka, *Comprehensive Nuclear Materials*, Elsevier, Radarweg 29, PO Box 211, 1000 AE Amsterdam, The Netherlands, 2012.
11 A. Courdouan, I. Christl, S. Meylan, P. Wersin and R. Kretzschmar, *Appl. Geochem.*, 2007, **22**, 1537–1548.
12 A. Courdouan, I. Christl, S. Meylan, P. Wersin and R. Kretzschmar, *Appl. Geochem.*, 2007, **22**, 2926–2939.
13 A. N. Vasiliev, N. L. Banik, R. Marsac, D. R. Froehlich, J. Rothe, S. N. Kalmykov and C. M. Marquardt, *Dalton Trans.*, 2015, **44**, 3837–3844.
14 G. R. Choppin, *J. Radioanal. Nucl. Chem.*, 2007, **273**, 695–703.
15 K. Maher, J. R. Bargar and G. E. Brown, Jr., *Inorg. Chem.*, 2013, **52**, 3510–3532.
16 T. Fanghänel and V. Neck, *Pure Appl. Chem.*, 2002, **74**, 1895–1907.
17 R. Guillaumont, T. Fanghänel, V. Neck, J. Fuger and D. A. Palmer, *Update on the Chemical Thermodynamics of Uranium, Neptunium, Plutonium, Americium and Technetium*, Elsvier B.V., 2003.
18 R. J. Lemire, *Chemical thermodynamics of neptunium and plutonium*, Elsevier, 2001.
19 W. Hummel, G. Anderegg, L. Rao, I. Puigdomenech and O. Tochiyama, Chemical Thermodynamics of Compounds and Complexes of U, Np, Pu, Am, Tc, Se, Ni and Zr with Selected Organic Ligands, Elsvier B.V., 2005.
20 J. J. Katz, G. T. Seaborg and L. R. Morss, *The Chemistry of the Actinide Elements*, Chapman and Hall, New York, 1986.
21 J. P. Kaszuba and W. H. Runde, *Environ. Sci. Technol.*, 1999, **33**, 4427–4433.
22 K. L. Nash, J. M. Cleveland and T. F. Rees, *J. Environ. Radioact.*, 1988, **7**, 131–157.
23 G. Bidoglio, A. Avogadro, A. De Plano and G. P. Lazzari, *Radiochim. Acta*, 1988, **44–45**, 29–32.
24 G. Bidoglio, A. De Plano, A. Avogadro and C. N. Murray, *Inorg. Chim. Acta*, 1984, **94**, 136–137.
25 P. Vitorge, H. Capdevila, S. Maillard, M.-H. Faure and T. Vercouter, *J. Nucl. Sci. Technol.*, 2014, **39**, 713–716.
26 K. Takao, S. Takao, A. C. Scheinost, G. Bernhard and C. Hennig, *Inorg. Chem.*, 2009, **48**, 8803–8810.
27 H. Stöber, PhD dissertation, Kernforschungszentrum Karlsruhe, 1972.
28 D. Fellhauer, J. Rothe, M. Altmaier, V. Neck, J. Runke, T. Wiss and T. Fanghänel, *Radiochim. Acta*, 2016, **104**, 355–379.
29 M. M. Maiwald, T. Sittel, D. Fellhauer, A. Skerencak-Frech and P. J. Panak, *J. Chem. Thermodyn.*, 2018, **116**, 309–315.
30 P. G. Hagan and J. M. Cleveland, *J. Inorg. Nucl. Chem.*, 1966, **28**, 2905–2909.
31 H. A. Friedman and L. M. Toth, *J. Inorg. Nucl. Chem.*, 1980, **42**, 1347–1349.
32 V. Neck, T. Fanghänel, G. Rudolph and J. I. Kim, *Radiochim. Acta*, 1995, **69**, 39–47.
33 C. Reichardt, *Chem. Rev.*, 1994, **94**, 2319–2358.
34 C. Reichardt, *Green Chem.*, 2005, **7**, 339.
35 S. J. Schmidtke Sobeck, *Chem. Educ.*, 2013, **18**, 99–103, p. 105.
36 C. Reichardt, *Angew. Chem., Int. Ed. Engl.*, 1965, **4**, 29–40.
37 C. Reichardt, *Angew. Chem., Int. Ed. Engl.*, 1979, **18**, 98–110.
38 M. Uematsu and E. U. Frank, *J. Phys. Chem. Ref. Data*, 1980, **9**, 1291–1306.
39 J. B. Hasted, D. M. Ritson and C. H. Collie, *J. Chem. Phys.*, 1948, **16**, 1–21.
40 A. Skerencak, P. J. Panak, W. Hauser, V. Neck, R. Klenze, P. Lindqvist-Reis and T. Fanghanel, *Radiochim. Acta*, 2009, **97**, 385–393.
41 A. Skerencak, P. J. Panak and T. Fanghänel, *Dalton Trans.*, 2013, **42**, 542–549.
42 D. R. Fröhlich, A. Skerencak-Frech and P. J. Panak, *Dalton Trans.*, 2014, **43**, 3958–3965.
43 A. Skerencak, S. Höhne, S. Hofmann, C. M. Marquardt and P. J. Panak, *J. Solution Chem.*, 2013, **42**, 1–17.
44 R. Smith, A. Martell and R. Motekaitis, NIST Critically Selected Stability Constants of Metal Complexes Database, 2004.
45 A. Skerencak-Frech, M. Maiwald, M. Trumm, D. R. Froehlich and P. J. Panak, *Inorg. Chem.*, 2015, **54**, 1860–1868.

 This journal is © The Royal Society of Chemistry and the Centre National de la Recherche Scientifique 2018